

Early Explorations of Lightweight Models for Wound Segmentation on Mobile Devices

Vanessa Borst(✉), Timo Dittus, Konstantin Müller, and Samuel Kounev

Software Engineering Group, University of Würzburg, Germany

✉ Corresponding author: vanessa.borst@uni-wuerzburg.de

Abstract. The aging population poses numerous challenges to health-care, including the increase in chronic wounds in the elderly. The current approach to wound assessment by therapists based on photographic documentation is subjective, highlighting the need for computer-aided wound recognition from smartphone photos. This offers objective and convenient therapy monitoring, while being accessible to patients from their home at any time. However, despite research in mobile image segmentation, there is a lack of focus on mobile wound segmentation. To address this gap, we conduct initial research on three lightweight architectures to investigate their suitability for smartphone-based wound segmentation. Using public datasets and UNet as a baseline, our results are promising, with both ENet and TopFormer, as well as the larger UNeXt variant, showing comparable performance to UNet. Furthermore, we deploy the models into a smartphone app for visual assessment of live segmentation, where results demonstrate the effectiveness of TopFormer in distinguishing wounds from wound-coloured objects. While our study highlights the potential of transformer models for mobile wound segmentation, future work should aim to further improve the mask contours¹.

Keywords: Medical Image Segmentation · Mobile AI · Deep Learning.

1 Introduction

Chronic wounds, such as diabetic foot ulcers, affect a significant proportion of the world's population and present a major challenge to healthcare systems worldwide. In the United States alone, it is estimated that more than 6 million people suffer from chronic wounds each year [23]. In addition to diabetes, age is a significant risk factor, with a disproportionate impact on the elderly. This is evidenced by a prevalence of 7.8% in German nursing home residents [24] compared to 1% in the German population [9]. As the world's population continues to age and the incidence of conditions such as diabetes increases, the prevalence of chronic wounds is expected to soar in the coming years. This increase poses a significant challenge to healthcare providers in providing appropriate care to those affected. From the patient's perspective, the need for frequent visits to specialised wound care facilities to manage chronic wounds can be a significant burden. Access to such clinics may be limited, particularly in remote areas, and

¹ This is an extended version of our KI 2024 paper, available at the Springer website.

mobility issues exacerbate the challenge. There is an urgent need for innovative solutions to alleviate these burdens and improve access to wound care services.

Telemedicine and automation offer promising ways to address these challenges by improving efficiency and accessibility. Automated wound size monitoring has the potential to eliminate the need for patients to visit clinics solely for monitoring purposes, thereby reducing the associated logistical challenges and relieving the burden on healthcare professionals. Furthermore, automated approaches provide timely and accurate information on wound status, facilitating proactive intervention. Mobile semantic segmentation emerges as a key technology in realizing these advancements, providing real-time feedback and segmentation masks directly to users, thereby circumventing latency issues associated with server-based processing. In addition, deploying models directly on smartphones ensures enhanced privacy and security by keeping sensitive medical data local. In addition, it enables offline functionality, which is crucial for applications in remote areas with limited network coverage. Despite the advantages of mobile segmentation, there are also significant challenges associated with this endeavour. To be effective, such solutions must include small, lightweight models that can be seamlessly deployed on smartphones. At the same time, such models must be robust in the face of challenging conditions such as different backgrounds, varying lighting conditions, and different camera settings, as mobile wound monitoring is intended to take place in the patient’s home environment.

However, despite the necessity for compact yet resilient models, the investigation into mobile wound segmentation remains limited to date. While several methods have been proposed for wound segmentation utilizing feature-engineering-based machine learning [27,35,14], deep learning [20,16,4,8], or even both [31,15], they often lack emphasis on lightweight architectures and mobile suitability. Some publications suggest that the analyzed architecture(s) could be used on mobile devices due to its efficiency, but such indications often rely solely on metrics such as parameter count as mobile performance indicator, lacking real-world deployment [33,20]. Of the few approaches deployed to a mobile device in practice, many apply traditional image processing rather than deep learning [25,30,7], while others evaluate only single architectures [19], or require manual annotation outlines from users [1,2]. To the best of our knowledge, a systematic comparison of different neural network-based wound segmentation techniques on mobile devices is still pending. In contrast, the number of proposed architectures for mobile segmentation beyond the wound context has increased significantly. To address this discrepancy, this work conducts initial investigations into the applicability of different architectures from non-wound domains for mobile wound segmentation, including a visual comparison in real-world usage.

2 Approach

2.1 Task Definition and Requirements

This study aims to assess the efficacy of lightweight models for mobile wound segmentation by systematically comparing approaches from beyond the wound

domain. In particular, we focus on their ability to perform live segmentation from smartphone camera streams, for which we consider the following requirements paramount: (i) **accuracy**: High segmentation performance for accurate analysis of wound area (ii) **efficiency**: Small number of parameters to enable mobile processing (iii) **robustness**: Effective performance under varying conditions for use in non-standardized home environments (iv) **practicality**: Effective segmentation in real-world deployment to enhance medical practice.

2.2 Model Selection

The number of proposed models for segmentation on mobile devices has increased significantly beyond wound segmentation. Notable advances include CNN-based methods, such as encoder-decoder architectures with lightweight backbones such as MobileNets [11,10] combined with different decoders, ENet [21], UNeXt [29], or Fast-SCNN [22], which have proven successful in mobile environments. In addition, vision transformer-based models, such as MobileFormer [3], MobileViT [17], Seaformer [32], or TopFormer [38], have been explored increasingly. From this spectrum, our model selection aims to cover different network types (CNN, vision transformer) and application domains (general-purpose, (bio)medicine), while setting reasonable limits on training effort. Therefore, we limit the inclusion of architectures to four, prioritizing the assessment of different-sized variants of selected methods where feasible. Specifically, we selected TopFormer [38], a representative (hybrid) vision transformer among recent general-purpose state-of-the-art (SOTA) methods, and UNeXt [29], a compact CNN-based SOTA technique for medical segmentation. The selection of these two SOTA models was based on the following criteria: (i) competitive performance on respective benchmark datasets (ii) publication in prestigious journals or conferences (iii) efficient resource utilization, as indicated by reported parameter counts and GFLOPs (iv) code availability on GitHub. Additionally, ENet [21], a widely referenced general-purpose CNN for real-time semantic segmentation from 2016, was included due to its remarkable efficiency in terms of trainable parameters and promising outcomes in medical segmentation studies [37,28], given its size. Lastly, to establish a baseline for wound segmentation, we integrated UNet [26], a prominent model in biomedical segmentation. Table 1 outlines the selection, with parameters reported in million (M) for binary segmentation (one out-channel).

Table 1: Overview of the included segmentation techniques.

	UNet [26]	ENet [21]	UNeXt [29]		TopFormer [38]		
			Base	Small	Base	Small	Tiny
Params	31.03M	0.35M	1.47M	0.25M	5.03M	3.01M	1.39M
Type	CNN	CNN	CNN		Hybrid CNN-ViT		
Domain	Biomedicine	General purpose	Medicine		General purpose		

3 Experimental Setup

3.1 Dataset

We perform experiments on a combination of two prominent datasets: the *Foot Ulcer Segmentation Challenge 2021 (FuSeg)* [34] and the *Diabetic Foot Ulcer Challenge 2022 (DFUC 2022)* [13,36] datasets. FuSeg encompasses 1,210 foot ulcer images, each with a resolution of 512×512 pixels, sourced from 889 patients’ medical visits spanning from October 2019 to April 2021. Meanwhile, the DFUC 2022 dataset comprises 4,000 foot ulcer images with a resolution of 640×480 pixels, captured approximately 30 to 40 cm away from the ulcer. Our custom dataset, *Combined Foot Ulcers (CFU)*, integrates FuSeg and DFUC 2022, comprising images with mixed resolutions of either 512×512 or 640×480 pixels. Due to the privacy of test set annotations (200 out of 1,210 for FuSeg and 2,000 out of 4,000 for DFUC 2022), only publicly accessible training and validation images are utilized for CFU. To prevent data leakage, duplicate images within FuSeg and DFUC 2022 were identified and removed. A similarity analysis, employing the perceptual hashing algorithm [18], was conducted. Image sets with identical raw bytes or perceptual hash values exhibiting a Hamming distance of 11 or less were deemed duplicates. For illustrative purposes, a number of examples are provided in Figure 2. Eliminating duplicate image-annotation pairs, we obtained a final dataset with 2,887 samples after discarding 123 pairs. Next, these samples were randomly partitioned into training (60%), validation (20%), and test (20%) set.

3.2 Evaluation Protocol

To assess model performance, we employed established segmentation metrics, such as Dice score (DSC), Intersection over Union (IoU), precision (Prc), and recall (Rec), utilizing the micro-averaging method while excluding the background class. Our analysis covered two training modalities: training models from scratch and utilizing pre-training on either the ImageNet [6] or Cityscapes [5] dataset. To facilitate this, we downloaded pre-trained weights where available: ENet (Cityscapes), UNet (ImageNet), and TopFormer (ImageNet). Since pre-trained weights were unavailable for UNeXt, we trained both variants ourselves for 100 epochs on Cityscapes, using the best checkpoints as initial weights.

3.3 Implementation Details

We implemented this approach using Python 3.10.9 and PyTorch 2.0.1 on a server with two partitioned Nvidia A100 GPUs, reserving a large-sized instance with 40 GB VRAM for our experiments. All models were trained end-to-end using the AdamW optimizer with an initial learning rate of 0.0001, a batch size of four, and the binary cross entropy (BCE) loss. We used a *ReduceLROnPlateau* scheduler conditioned on the Dice score, with a minimum learning rate of 0.000001. All models were trained for 200 epochs from scratch and for at least

130 epochs in the pre-training setting. For both, the best checkpoints, according to the mean IoU on the validation set, were used for the ensuing test set evaluation. All images were resized to 512×512 pixels and normalized during training. We applied thresholding to annotated masks to eliminate out-of-class pixels and used the following data augmentations for each training set sample: Gaussian blur with a kernel size of 25 and a randomly sampled standard deviation from a uniform distribution of $[0.001, 2.0]$, random affine transforms (incl. translations by up to 12.5%, rotations by up to 180 degrees, scaling between 50% and 150% of the original size, and shear of up to 22.5 degrees), color jitter, as well as random horizontal and vertical flips, each with a 50% probability. Details about the augmentations can be found in the example configuration file of Listing 1.1.

4 Evaluation

4.1 Results

We compare the selected models in Table 2, where we report the micro-averaged metric scores of each variant for both training modalities. Our findings indicate that, without pretraining, UNeXt-B exhibits the most favorable segmentation performance, balancing parameter count and segmentation quality. Notably, all lightweight models, except UNeXt-S, achieve results within a similar size range as the larger UNet, with the base variants of both UNeXt and Topformer, and ENet even slightly surpassing UNet. Pretraining considerably enhances performance across all models in terms of IoU and DSC metrics. Specifically, all lightweight networks demonstrate comparable performance, with IoU ranging from 69% to 72% and DSC from 82% to 84%, except for UNeXt-S, which performs worse.

Table 2: Comparison of all models on the CFU dataset. The micro-averaged metrics (in %) were calculated on the test set. Parameters are reported in millions.

Model	Without pretraining				With pretraining				Params↓
	IoU	DSC	Prc	Rec	IoU	DSC	Prc	Rec	
U-Net	65.69	79.30	81.57	77.14	74.69	85.56	87.74	83.39	31.03M
TopFormer-B	66.10	79.59	86.63	73.61	72.41	84.00	84.56	83.44	5.03M
TopFormer-S	63.36	77.57	83.31	72.57	71.56	83.42	85.95	81.04	3.01M
UNeXt-B	68.96	81.63	88.49	75.76	70.12	82.43	87.40	78.01	1.47M
TopFormer-T	62.51	76.93	84.27	70.77	69.62	82.09	83.90	80.36	1.39M
ENet	67.27	80.43	89.21	72.23	71.71	83.52	89.98	77.93	0.35M
UNeXt-S	59.16	74.34	77.52	71.41	64.13	78.14	87.52	70.58	0.25M

4.2 Real-World Deployment

To assess the models' real-world capabilities, we developed a Flutter prototype. For seamless integration within the app, all PyTorch models except UNet were

converted to TorchScript by tracing. The deployed networks performed live segmentation of camera streams, with center-cropped images to 224×224 pixels for efficient processing. Following preliminary trials, a prediction threshold of 0.75 was established for the derivation of binary masks, with the objective of achieving more precise segmentations and reduced jitter during inference. We rigorously tested the architectures on an *OnePlus 7 Pro* Android phone from 2019. All models ran smoothly without stalling, demonstrating the feasibility of mobile segmentation using Flutter. To enable visual assessments, we devised six distinct scenes and captured live segmentations via screenshots, utilizing the variants with pretraining. The scenes encompass: (i) a neutral environment devoid of objects (ii) two diverse wound images not from the CFU dataset (iii) two scenes featuring everyday objects with colors resembling wounds (iv) a scene with two everyday objects, one of which has a wound-like color. The resulting segmentation masks generated by the models are depicted in Figure 1. Visually, ENet exhibits the worst results among the tested models, with pixelated and holey masks as well as inaccuracies such as falsely identifying everyday objects, including the blue sponge. In contrast, the TopFormer and UNeXt variants show more promising results, identifying wounds with fewer imperfections, albeit with somewhat indistinct edges and contours. Notwithstanding the recognition difficulties encountered by the UNeXt models when presented with objects of wound-like colours, there is an overall improvement for both architectures compared to ENet. Overall, the TopFormer-based networks appear to be superior, as they proved quite effective at distinguishing between wounds and wound-coloured objects. Notably, the smallest variant (TF-T) performs exceptionally well in our example scenes, while the CNN-based UNeXt-B, despite exhibiting promising performance in Table 2, displays significantly poorer performance.

5 Conclusion and Future Work

In conclusion, our preliminary investigations into lightweight neural networks demonstrate their potential for mobile wound segmentation. The analyzed architectures, especially TopFormer, yield promising results in real-world application scenarios, although some refinements are still necessary, such as clearer edge detection. Future work will include extending the comparison to further promising architectures such as MBSNet [12], MobileFormer [3], or Seaformer [32]. Furthermore, retraining the networks on an expanded dataset with more images, including those featuring objects with wound-similar colors, is expected to enhance the robustness and generalization ability of the models, thereby improving the accessibility and effectiveness of future wound care.

Acknowledgments. We thank Adrian Strutt for conducting preliminary experiments.

Disclosure of Interests. The authors have no competing interests to declare.

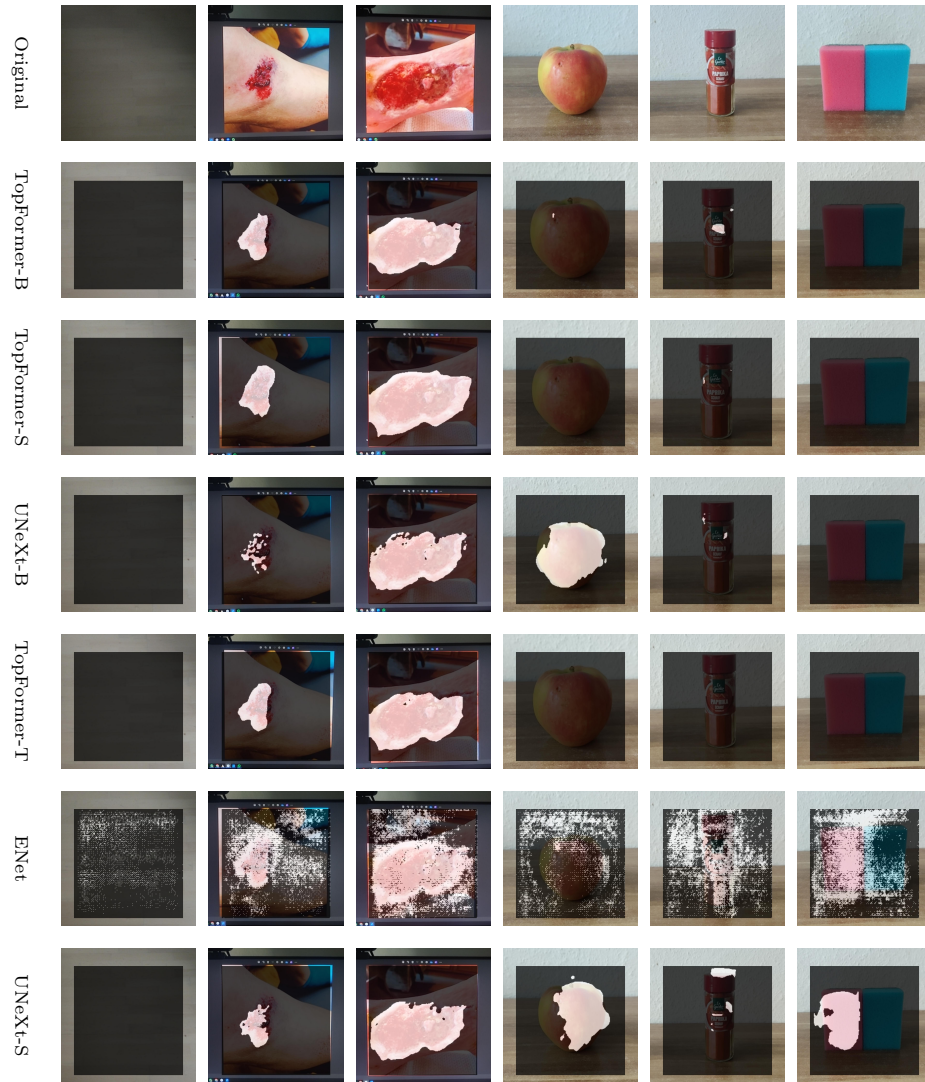


Fig. 1: Live segmentation of different model variants in our mobile app, arranged in descending order of parameter count.

A Appendix

Examples from FuSeg



0111.png

0386.png



0161.png

0163.png



0318.png

0415.png

Examples from DFUC



100475.jpg

100511.jpg



101502.jpg

101941.jpg



100480.jpg

100516.jpg

Fig. 2: Examples of identical or highly similar image pairs from both datasets.

Listing 1.1: Example configuration for E-Net (pre-trained)

```

architecture:
  arch_type: "ENetV2"
  model_name: "ENetV2-CFU-512-
              pretrained"
  in_size: 512
  use_pretrained: True
settings:
  max_epochs: 200
  batch_size: 4
  random_seed: 42
  full_determinism: True
  mixed_precision: True
  torch_compile: False
  num_workers: 4
  pin_memory: True
  checkpoints:
    save_mode: "best"
    metric: "iou"
    min_epoch: 30
  save_sample_segmentations:
    False
  transforms_backend: "
    torchvision"
optimizer:
  type: "AdamW"
  lr: 0.0001
loss:
  type: "default"
scheduler:
  type: "reduce_lr_on_plateau"
  metric: "dice"
  mode: "max"
  min_lr: 0.000001
  factor: 0.5
  verbose: True
  early_stop: False
metrics:
  tracked:
    - "dice"
    - "iou"
    - "precision"
    - "recall"
  averaging_method: "micro"
  ignore_background_class: True
dataset:
  type: "CFU"
transforms:
  train:
    - to_tensor: True
    - pad_and_resize:
      size: 512
    - gaussian_blur:
      kernel_size: 25
      sigma: (0.001, 2.0)
    - threshold:
      threshold: 127
      pixel_min: 0
      pixel_max: 255
      apply_to_mask: True
      apply_to_image: False
    - color_jitter:
      brightness: 0.4
      contrast: 0.5
      saturation: 0.25
      hue: 0.01
    - normalize:
      mean: [ 0.5, 0.5, 0.5 ]
      std: [ 0.5, 0.5, 0.5 ]
    - random_horizontal_flip:
      p: 0.5
    - random_vertical_flip:
      p: 0.5
    - random_affine:
      degrees: (-180, 180)
      translate: (0.125, 0.125)
      scale: (0.5, 1.5)
      shear: 22.5
      fill: -1.0
      mask_fill: 0
  val:
    - to_tensor: True
    - pad_and_resize:
      size: 512
    - threshold:
      threshold: 127
      pixel_min: 0
      pixel_max: 255
      apply_to_mask: True
      apply_to_image: False
    - normalize:
      mean: [ 0.5, 0.5, 0.5 ]
      std: [ 0.5, 0.5, 0.5 ]
  test:
    - to_tensor: True
    - pad_and_resize:
      size: 512
    - threshold:
      threshold: 127
      pixel_min: 0
      pixel_max: 255
      apply_to_mask: True
      apply_to_image: False
    - normalize:
      mean: [ 0.5, 0.5, 0.5 ]
      std: [ 0.5, 0.5, 0.5 ]

```

References

1. Cazzolato, M.T., Ramos, J.S., Rodrigues, L.S., Scabora, L.C., Chino, D.Y., Jorge, A.E., Azevedo-Marques, P.M., Traina, C., Traina, A.J.: Semi-automatic ulcer segmentation and wound area measurement supporting telemedicine. In: 2020 IEEE 33rd International Symposium on Computer-Based Medical Systems (CBMS). pp. 356–361. IEEE (2020)
2. Cazzolato, M.T., Ramos, J.S., Rodrigues, L.S., Scabora, L.C., Chino, D.Y., Jorge, A.E., de Azevedo-Marques, P.M., Traina Jr, C., Traina, A.J.: The utrack framework for segmenting and measuring dermatological ulcers through telemedicine. *Computers in Biology and Medicine* **134**, 104489 (2021)
3. Chen, Y., Dai, X., Chen, D., Liu, M., Dong, X., Yuan, L., Liu, Z.: Mobile-former: Bridging mobilenet and transformer. In: Proceedings of the IEEE/CVF conference on computer vision and pattern recognition. pp. 5270–5279 (2022)
4. Chino, D.Y., Scabora, L.C., Cazzolato, M.T., Jorge, A.E., Traina-Jr, C., Traina, A.J.: Segmenting skin ulcers and measuring the wound area using deep convolutional networks. *Computer methods and programs in biomedicine* **191**, 105376 (2020)
5. Cordts, M., Omran, M., Ramos, S., Rehfeld, T., Enzweiler, M., Benenson, R., Franke, U., Roth, S., Schiele, B.: The cityscapes dataset for semantic urban scene understanding. In: Proceedings of the IEEE conference on computer vision and pattern recognition. pp. 3213–3223 (2016)
6. Deng, J., Dong, W., Socher, R., Li, L.J., Li, K., Fei-Fei, L.: Imagenet: A large-scale hierarchical image database. In: 2009 IEEE conference on computer vision and pattern recognition. pp. 248–255. Ieee (2009)
7. Ferreira, F., Pires, I.M., Ponciano, V., Costa, M., Villasana, M.V., Garcia, N.M., Zdravevski, E., Lameski, P., Chorbev, I., Mihajlov, M., et al.: Experimental study on wound area measurement with mobile devices. *Sensors* **21**(17), 5762 (2021)
8. Goyal, M., Yap, M.H., Reeves, N.D., Rajbhandari, S., Spragg, J.: Fully convolutional networks for diabetic foot ulcer segmentation. In: 2017 IEEE international conference on systems, man, and cybernetics (SMC). pp. 618–623. IEEE (2017)
9. Heyer, K., Herberger, K., Protz, K., Glaeske, G., Augustin, M.: Epidemiology of chronic wounds in germany: analysis of statutory health insurance data. *Wound Repair and Regeneration* **24**(2), 434–442 (2016)
10. Howard, A., Sandler, M., Chu, G., Chen, L.C., Chen, B., Tan, M., Wang, W., Zhu, Y., Pang, R., Vasudevan, V., et al.: Searching for mobilenetv3. In: Proceedings of the IEEE/CVF international conference on computer vision. pp. 1314–1324 (2019)
11. Howard, A., Zhmoginov, A., Chen, L.C., Sandler, M., Zhu, M.: Inverted residuals and linear bottlenecks: Mobile networks for classification, detection and segmentation. In: Proc. CVPR. pp. 4510–4520 (2018)
12. Jin, S., Yu, S., Peng, J., Wang, H., Zhao, Y.: A novel medical image segmentation approach by using multi-branch segmentation network based on local and global information synchronous learning. *Scientific Reports* **13**(1), 6762 (2023)
13. Kendrick, C., Cassidy, B., Pappachan, J.M., O’Shea, C., Fernandez, C.J., Chacko, E., Jacob, K., Reeves, N.D., Yap, M.H.: Translating clinical delineation of diabetic foot ulcers into machine interpretable segmentation. arXiv preprint arXiv:2204.11618 (2022)
14. Kolesnik, M., Fexa, A.: Multi-dimensional color histograms for segmentation of wounds in images. In: Image Analysis and Recognition: Second International Conference, ICIAR 2005, Toronto, Canada, September 28-30, 2005. Proceedings 2. pp. 1014–1022. Springer (2005)

15. Li, F., Wang, C., Liu, X., Peng, Y., Jin, S.: A composite model of wound segmentation based on traditional methods and deep neural networks. *Computational intelligence and neuroscience* **2018** (2018)
16. Liu, X., Wang, C., Li, F., Zhao, X., Zhu, E., Peng, Y.: A framework of wound segmentation based on deep convolutional networks. In: 2017 10th international congress on image and signal processing, biomedical engineering and informatics (CISP-BMEI). pp. 1–7. IEEE (2017)
17. Mehta, S., Rastegari, M.: Mobilevit: Light-weight, general-purpose, and mobile-friendly vision transformer. In: *International Conference on Learning Representations* (2021)
18. Micikevicius, P., Narang, S., Alben, J., Diamos, G., Elsen, E., Garcia, D., Ginsburg, B., Houston, M., Kuchaiev, O., Venkatesh, G., et al.: Mixed precision training. In: *International Conference on Learning Representations* (2018)
19. Ong, E.P., Yin, C.T.K., Lee, B.H.: Efficient deep learning-based wound-bed segmentation for mobile applications. In: 2020 42nd Annual International Conference of the IEEE Engineering in Medicine & Biology Society (EMBC). pp. 1654–1657. IEEE (2020)
20. Oota, S.R., Rowtula, V., Mohammed, S., Liu, M., Gupta, M.: Wsnet: towards an effective method for wound image segmentation. In: *Proceedings of the IEEE/CVF Winter Conference on Applications of Computer Vision*. pp. 3234–3243 (2023)
21. Paszke, A., Chaurasia, A., Kim, S., Culurciello, E.: Enet: A deep neural network architecture for real-time semantic segmentation. *arXiv preprint arXiv:1606.02147* (2016)
22. Poudel, R.P.K., Liwicki, S., Cipolla, R.: Fast-scnn: Fast semantic segmentation network. In: *30th British Machine Vision Conference 2019, BMVC 2019, Cardiff, UK, September 9-12, 2019*. BMVA Press (2019)
23. Powers, J.G., Higham, C., Broussard, K., Phillips, T.J.: Wound healing and treating wounds: Chronic wound care and management. *Journal of the American Academy of Dermatology* **74**(4), 607–625 (2016)
24. Raeder, K., Jachan, D.E., Müller-Werdan, U., Lahmann, N.A.: Prevalence and risk factors of chronic wounds in nursing homes in germany: a cross-sectional study. *International wound journal* **17**(5), 1128–1134 (2020)
25. Rocha, C.D.F.D., Carvalho, B.S., Marques, V.G., Silva, B.M.: Woundarch: A hybrid architecture system for segmentation and classification of chronic wounds. In: *Proceedings of the 14th International Joint Conference on Biomedical Engineering Systems and Technologies*. pp. 651–658. INSTICC, SciTePress (2021)
26. Ronneberger, O., Fischer, P., Brox, T.: U-net: Convolutional networks for biomedical image segmentation. In: *Medical image computing and computer-assisted intervention—MICCAI 2015: 18th international conference, Munich, Germany, October 5-9, 2015, proceedings, part III 18*. pp. 234–241. Springer (2015)
27. Song, B., Sacan, A.: Automated wound identification system based on image segmentation and artificial neural networks. In: *2012 IEEE International Conference on Bioinformatics and Biomedicine*. pp. 1–4. IEEE (2012)
28. Song, E., Zhan, B., Liu, H.: Combining external-latent attention for medical image segmentation. *Neural Networks* **170**, 468–477 (2024)
29. Valanarasu, J.M.J., Patel, V.M.: Unext: Mlp-based rapid medical image segmentation network. In: *International conference on medical image computing and computer-assisted intervention*. pp. 23–33. Springer (2022)
30. Varma, A., Varma, A., Jakkampudi, H.M., Raj, A.N.J.: Vision based pus segmentation and area estimation of wound using android application. *Indian Journal of Science and Technology* (2016)

31. Wagh, A., Jain, S., Mukherjee, A., Agu, E., Pedersen, P.C., Strong, D., Tulu, B., Lindsay, C., Liu, Z.: Semantic segmentation of smartphone wound images: Comparative analysis of ahrf and cnn-based approaches. *IEEE Access* **8**, 181590–181604 (2020)
32. Wan, Q., Huang, Z., Lu, J., Yu, G., Zhang, L.: Seaformer: Squeeze-enhanced axial transformer for mobile semantic segmentation. In: *International Conference on Learning Representations (ICLR)* (2023)
33. Wang, C., Anisuzzaman, D., Williamson, V., Dhar, M.K., Rostami, B., Niezgoda, J., Gopalakrishnan, S., Yu, Z.: Fully automatic wound segmentation with deep convolutional neural networks. *Scientific reports* **10**(1), 21897 (2020)
34. Wang, C., Mahbod, A., Ellinger, I., Galdran, A., Gopalakrishnan, S., Niezgoda, J., Yu, Z.: Fuseg: The foot ulcer segmentation challenge. *Information* **15**(3), 140 (2024)
35. Wang, L., Pedersen, P.C., Agu, E., Strong, D.M., Tulu, B.: Area determination of diabetic foot ulcer images using a cascaded two-stage svm-based classification. *IEEE Transactions on Biomedical Engineering* **64**(9), 2098–2109 (2016)
36. Yap, M.H., Cassidy, B., Byra, M., Liao, T.y., Yi, H., Galdran, A., Chen, Y.H., Brüngel, R., Koitka, S., Friedrich, C.M., et al.: Diabetic foot ulcers segmentation challenge report: Benchmark and analysis. *Medical Image Analysis* **94**, 103153 (2024)
37. Yuan, F., Zhang, Z., Fang, Z.: An effective cnn and transformer complementary network for medical image segmentation. *Pattern Recognition* **136**, 109228 (2023)
38. Zhang, W., Huang, Z., Luo, G., Chen, T., Wang, X., Liu, W., Yu, G., Shen, C.: Topformer: Token pyramid transformer for mobile semantic segmentation. In: *Proceedings of the IEEE/CVF Conference on Computer Vision and Pattern Recognition*. pp. 12083–12093 (2022)